Fish and Shellfish Immunology 93 (2019) 977–985

Contents lists available at ScienceDirect

Fish and Shellfish Immunology

journal homepage: www.elsevier.com/locate/fsi

Full length article

Identification and functional characterization of a C-type lectin gene from *Litopenaeus vannamei* that is associated with ER-stress response

Fei Song[a], Guo-Liang Chen[a], Ke-Cheng Lu[a], Jin-Quan Fan[a], Mu-Ting Yan[2], Hong-Hui He[c], Yu-Ying Lian[c], Chao-Zheng Zhang[d], Yi-Hong Chen[a,*]

[a] Institute of Modern Aquaculture Science and Engineering (IMASE), Guangzhou Key Laboratory of Subtropical Biodiversity and Biomonitoring, Guangdong Provincial Key Laboratory for Healthy and Safe Aquaculture, College of Life Science, South China Normal University, Guangzhou, 510631, PR China
[2] College of Marine Sciences, South China Agricultural University, Guangzhou, 510642, China
[c] State Key Laboratory for Biocontro, School of Life Sciences, Sun Yat-sen University, 135 Xingang Road West, Guangzhou, 510275, PR China
[d] Guangdong Provincial Center for Disease Control and Prevention, 160 QunXian Road, Guangzhou, 511430, PR China

ARTICLE INFO

Keywords:
ER-Stress
Unfolded protein response
C-type lectin
Litopenaeus vannamei

ABSTRACT

C-type lectins (CTLs), which bind carbohydrates in a Ca^{2+}-dependent manner, are involved in many cellular activities, especially immunity. CTLs play important roles in both the antibacterial and the antiviral immune response and are also associated with autoimmunity. Several CTLs have been investigated in crustaceans, primarily with respect to their function in the immune response. In this study, we cloned a novel *CTL* gene (*LvCTLU*) from *Litopenaeus vannamei*. LvCTLU is involved in microbe agglutination and phagocytosis. Downregulating *LvCTLU* increased the cumulative mortality of *L. vannamei* after *Vibrio parahemolyticus* infection. Similar to other reported CTLs, LvCTLU also had antiviral properties. Downregulation of *LvCTLU* also increased the cumulative mortality of *L. vannamei* after infection with white spot syndrome virus. More importantly, LvCTLU expression was induced by the unfolded protein response (UPR), which is the key pathway in the endoplasmic reticulum (ER)-stress response of eukaryotic organism. Our results suggested that this protein might be involved in the shrimp ER-stress response. Reporter gene assay indicated that *LvCTLU* was regulated by X-box-binding protein 1, which is the key transcription factor in the UPR. Our study thus revealed that LvCTLU plays vital roles in both the anti-pathogen immune response and the ER-stress response.

1. Introduction

Lectins, proteins that bind carbohydrates or glycoproteins without the involvement of enzymes, occur ubiquitously in animals, plants, and microorganisms [1]. Based on structural characteristics, calcium ion dependence, and the types of carbohydrates recognized, animal lectins can be grouped into four categories: C-type lectins (CTLs), P-type lectins, S-type lectins, and I-type lectins [2]. In general, lectins are associated with the regulation of cell adhesion and glycoprotein synthesis; the binding of soluble extracellular and intercellular glycoproteins; and the recognition of galactose residues and hydrolytic enzymes [3]. As lectins are highly selective, they are important in a variety of cellular physiological processes, particularly the innate immune response [4]. However, some lectins may also mediate the attachment and binding of bacteria and viruses to their intended targets [5,6].

CTLs are the most well-studied group of lectins. Lectins in the CTL superfamily have structurally homologous carbohydrate-recognition domains and often bind to carbohydrates in a Ca^{2+}-dependent fashion [7]. Based on additional non-lectin domains and overall gene structure, CTLs can be further subdivided into seven groups: hyalectans, asialoglycoprotein receptors, collectins, selectins, NK-group transmembrane receptors, macrophage mannose receptors, and simple (single domain) lectins [8]. CTLs are associated with a diverse range of functions, including cell-cell adhesion, the immune response to pathogens, and apoptosis [9].

CTLs may also be involved in stress responses or oxidative stress resistance. For example, a CTL mannose-binding protein in the lectin complement pathway (LCP) mediates complement activation after tissue oxidative stress [10], while the CTL Reg3α (HIP/PAP) suppressed extracellular oxidative stress in a murine model of acute liver failure [11]. CTLs are also associated with other stress responses: the sialic acid-binding lectin (leczyme) in bullfrog eggs activated endoplastic recticulum (ER)-stress-mediated apoptosis [12], and transcriptome analyses showed that some CTLs were expressed in response to salinity

* Corresponding author.
E-mail address: 20181024@m.scnu.edu.cn (Y.-H. Chen).

https://doi.org/10.1016/j.fsi.2019.08.056
Received 5 June 2019; Received in revised form 17 August 2019; Accepted 22 August 2019
Available online 23 August 2019

stress in the pacific oyster *Crassostrea gigas* [13].

Due to the great economic value of shrimp aquaculture and the severe threats posed to this industry by pathogenic infection and environmental stressors, many studies have focused on shrimp immune responses and stress resistance mechanisms [CITE]. In particular, several recent studies have investigated the function of shrimp CTLs; most of these specifically concentrated on the functions of CTLs in innate immunity. For example, galactose-binding CTLs carrying two glutamine-proline-aspartate motifs were isolated from the hemocytes of *Fenneropenaeus merguiensis* and shown to participate in immune defense, while in red swamp crayfish, a CTL was identified that acted as both an antibacterial and an antiviral [14,15]. Other studies have suggested that shrimp lectins may also be involved in the resistance to environmental stressors, including high ammonia levels, low temperatures, and low salinities [16,17]. However, the underlying mechanisms by which shrimp lectins respond to environmental stressors remain unclear. Here, we show that a *Litopenaeus vannamei* CTL (LvCTLU) not only participates in the response to pathogen infection but is also activated downstream of the unfolded protein response (UPR), which is a key pathway conferring environmental stress resistance on *L. vannamei* [18–20].

2. Materials and methods

2.1. Subcellular localization of LvCTLU

Drosophila Schneider 2 (S2) cell maintenance and DNA transfection were performed as previously described [21]. To perform subcellular localization, the enhanced green fluorescent protein (eGFP)-fused protein expression vector for LvCTLU (1–170 aa) was constructed by inserting the corresponding DNA fragment into the recombinant vector pAC-eGFP (the primers used are listed in Table 1). At 48 h post-transfection, the cells on the coverslips were washed twice with PBS and stained with Hoechst 33258 solution (Beyotime, China). The cells were then observed using a laser scanning confocal microscope (Leica, Germany).

2.2. Dual-luciferase reporter gene assay

The *LvCTLU* promoter, which was obtained from the *L. vannamei* Genome Sequencing Project (GenBank assembly accession: GCA_002993835.1), was 669 bp in length. Reporter gene vectors were constructed based on pGL4-Basic (Promega, USA), and PCR products were amplified (using the primers listed in Table 1). The expression vector encoding the splicing form of *L. vannamei* XBP1 (LvXBP1s) was constructed as described previously [18]. The S2 cells were cultured at 28 °C with Schneider Insect Medium (Sigma) supplemented with 10% FBS in 96-well plates for 24 h. Then, 50 ng of firefly luciferase reporter gene plasmid, 15 ng of pRL-TK renilla luciferase plasmid, and 50 ng of expression plasmid (the pAC5.1-Basic plasmid was used as the negative control) were transfected into S2 cells in a single well using FuGENE 6 Transfection Reagent (Promega, USA), following the manufacturer's instructions, and fluorescence intensity was measured at 48 h post-transfection. All experiments were repeated three times. The expression of pAC-LvXBP1s was detected by western-blot analyses with anti-V5 monoclonal antibody (CST, USA), and horseradish peroxidase (HRP)-conjugated goat anti-mouse IgG antibody (Pierce, USA). Signal is detected with a SuperSignal West Pico Trial Kit (Pierce).

2.3. Synthesis of double-stranded RNAs

The DNA templates of *LvCTLU* double strand RNA (designated dsLvCTLU) were PCR amplified using the primer pairs DsRNA-dsLvCTLU-T7-F/DsRNA-dsLvCTLU-R and DsRNA-dsLvCTLU-F/DsRNA-dsLvCTLU-T7-R (Table 1). The PCR products were used as RNA templates and subjected to *in vitro* transcription and purification using RiboMAXTM Large-Scale RNA Production System-T7 (Promega, USA), following the manufacturer's protocols. dsLvCTLU was 541 bp in length. DNA templates for the synthesis of *eGFP* dsRNA (dseGFP) and *L. vannamei* immunoglobulin heavy chain binding protein dsRNA (dsLvBip) were prepared as previously described [22].

Table 1
Summary of primers used in this study.

Primers	Sequence (5′-3′)
For cDNA cloning	
LvCTLU-5RACE1	CAGTTGTAACTTCAAAGAAACTCGGAGG
LvCTLU-5RACE2	GGTAGTACATGGAGCACTGTTTACTTCTAAGC
LvCTLU-3RACE1	GAAACGTGCATTGGCCTGAGCGACAGCA
LvCTLU-3RACE2	ACTTGGCTTCCCTCGACTCCACGGCGCA
For genes expression[a]	
pAC-eGFP-Kpn I-F	ATA**GGTACC**ATGGTGAGCAAGGGCGAGG
p AC-eGFP-EcoR I-R	TTA**GAATTC**ACCTTGTACAGCTCGTCCATGC
p AC-LvCTLU-Xba I-F	CGG**GGTCTAGA**GATGTATCGTCTGGAAAGATTACTCA
p AC-LvCTLU-SacII-R	CGG**CCGCGG** CTTCTGTGGGTAAGCCCTGCACA
pET32a-LvCTLU-Kpn I-F	TAT**GGTACC**CAGTGCCCCGATACCTTCTT
pET32a-LvCTLU-EcoR I-R	TTA**GAATTC**CTTCTGTGGGTAAGCCCTGCAC
For real-time RT-PCR	
QPCR- LvCTLU-F	GTCGTAGACACCGGCGACAC
QPCR- LvCTLU-R	GGGAAGCCAAGTCCACAGTCC
QPCR-LvEF1a-F	GCTGATTGCGCCGTACTCAT
QPCR-LvEF1a-R	TCACGGGTCTGTCCGTTCTT
For dsRNA templates amplification	
DsRNA-LvCTLU-541-T7-F1	GGATCCTAATACGACTCACTATAGGGTGCAGGGCTTACCCACAGA
DsRNA-LvCTLU-541-R1	GCACCATTCCCAGTCTCACA
DsRNA-LvCTLU-541-F2	GTGCAGGGCTTACCCACAGA
DsRNA-LvCTLU-541-T7-R2	GGATCCTAATACGACTCACTATAGGGCACCATTCCCAGTCTCACA
For reporter gene assay[b]	
pGL3-CTLU-Kpn I-F	ATT**GGTACC**GCACGTGTGTGATTATATACATTTG
pGL3-CTLU-Bgl I-R	CCG**AGATCT**GGTCCCGGCCACGGCGATAGC
pGL3-CTLUmATF/CRE-F	gtcatgacACAACTATGGCCATTAGGAGCGT
pGL3-CTLUmATF/CRE-R	TGACGTGACAGAAAAGAAATCAATA

[a] Nucleotides in bold indicate restriction sites introduced for clonin
[b] Nucleotides in lower-case are the mutant sites.

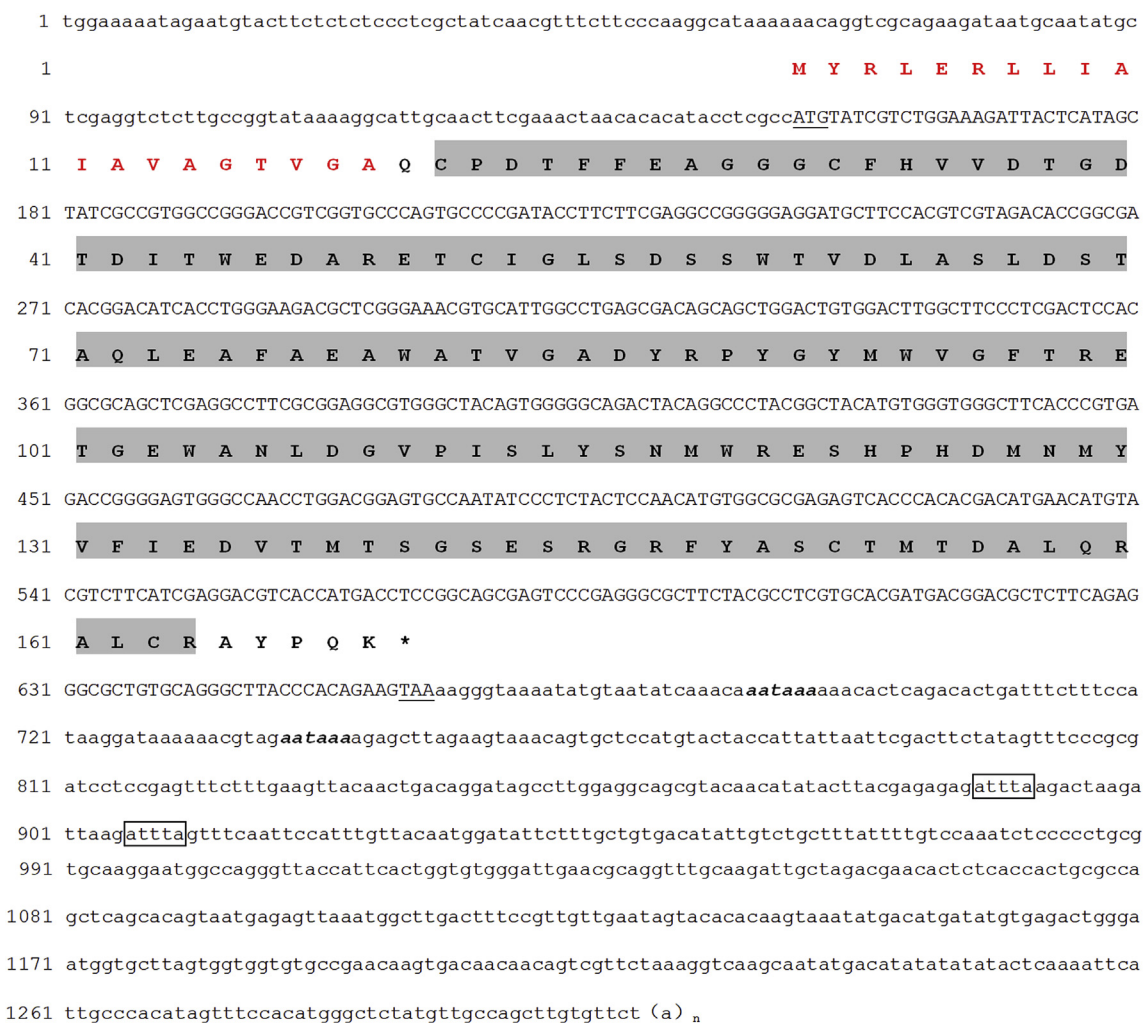

Fig. 1. Nucleotide and deduced amino acid sequence of *LvCTLU*. The ORFs of the nucleotide sequences are shown in uppercase letters; the 5′- and 3′-UTRs are shown in lowercase letters. Nucleotides and amino acids are numbered on the left of the sequences. The conserved domains were shaded, and signal peptide was colored red. The conserved domains are shaded. The poly (A) signals (aataaa) were italic representation. The 3′-UTR instability motifs (attta) were boxed. (For interpretation of the references to color in this figure legend, the reader is referred to the Web version of this article.)

2.4. Pathogenic challenge, UPR activation, and the preparation of templates for real-time RT-PCR

L. vannamei were raised in a shrimp farm in Guangzhou City, Guangdong Province, China. Healthy shrimp (~6 g) were collected and acclimated in a recirculating water tank system filled with air-pumped seawater (4.5% salinity) at ~28 °C. Shrimp were allowed to acclimatize for at least one week before experimentation. To investigate the gene expression profiles of *LvCTLU* in shrimp infected with white spot syndrome virus (WSSV) or *Vibrio parahaemolyticus,* healthy *L. vannamei* were injected intramuscularly at the second abdominal segment with 50 μL WSSV inoculum (~10^5 virions) or 50 μL of *V. parahaemolyticus* (7.0×10^5 CFU/g). Gills, intestine and hepatopancreas from five shrimp infected with WSSV were collected at 0, 6, 12, 24, 36, 48, 72 and 96 h post-infection (hpi); gills, intestine and hepatopancreas from five shrimp infected with *V. parahemolyticus* were collected at 0, 6, 12, 24, 36 and 72 hpi were pooled together as one sample. Samples from five shrimps were injected with PBS and used as the control.

To investigate UPR activation, 150 healthy *L. vannamei* were intramuscularly injected at the second abdominal segment with 6 μg dsLvBip or 6 μg dseGFP (control) in a total volume of 50 μL. Total RNA from the hemocytes of each injected shrimp was isolated at 0, 4, 8, 12, 24, 36, 48, 72, and 96 h post-injection. At each time point for each type of injection, hemocytes from five shrimp were pooled. Each data point represented three parallel samples.

Total RNA was extracted using RNeasy Mini Kits (Qiagen, Germany) and reverse transcribed into cDNA using PrimeScript RT Reagent Kits (TaKaRa, Japan). Real-time RT-PCR assays were performed with a LightCycler 480 System (Roche, Germany). The results were calculated using the $2^{-\Delta\Delta Ct}$ method after normalization to *LvEF-1a* (GenBank Accession No. GU136229).

2.5. Analysis of the microbe agglutinating specificity of LvCTLU

Gram-negative bacteria (*V. parahaemolyticus*) and gram-positive bacteria (*Streptococcus agalactiae*) were labeled with 5 μg/mL fluorescein isothiocyanate (FITC) and resuspended in TBS-Ca buffer (50 mM Tris-HCl, 100 mM NaCl, 10 mM $CaCl_2$, pH 7.5) to a density of 10^6 CFU/mL. Next, 10 μL of each bacteria suspension was mixed with either 20 μL of signal-peptide-free LvCTLU (0.1 mg/mL) or 20 μL of the control protein (0.1 mg/mL; a 21-kDa 6×His fusion protein expressed by the pET32a vector). The mixtures were incubated at 25 °C for 1 h. The agglutination of FITC-labeled cells was observed with a TE2000 microscope (Nikon, Japan) at 488 nm. To determine whether the observed agglutination was calcium-dependent, FITC-labeled microbes were incubated with LvCTLU in TBS-EDTA buffer (50 mM Tris-HCl, 100 mM NaCl, 4 mM EDTA, pH 7.5) as described above.

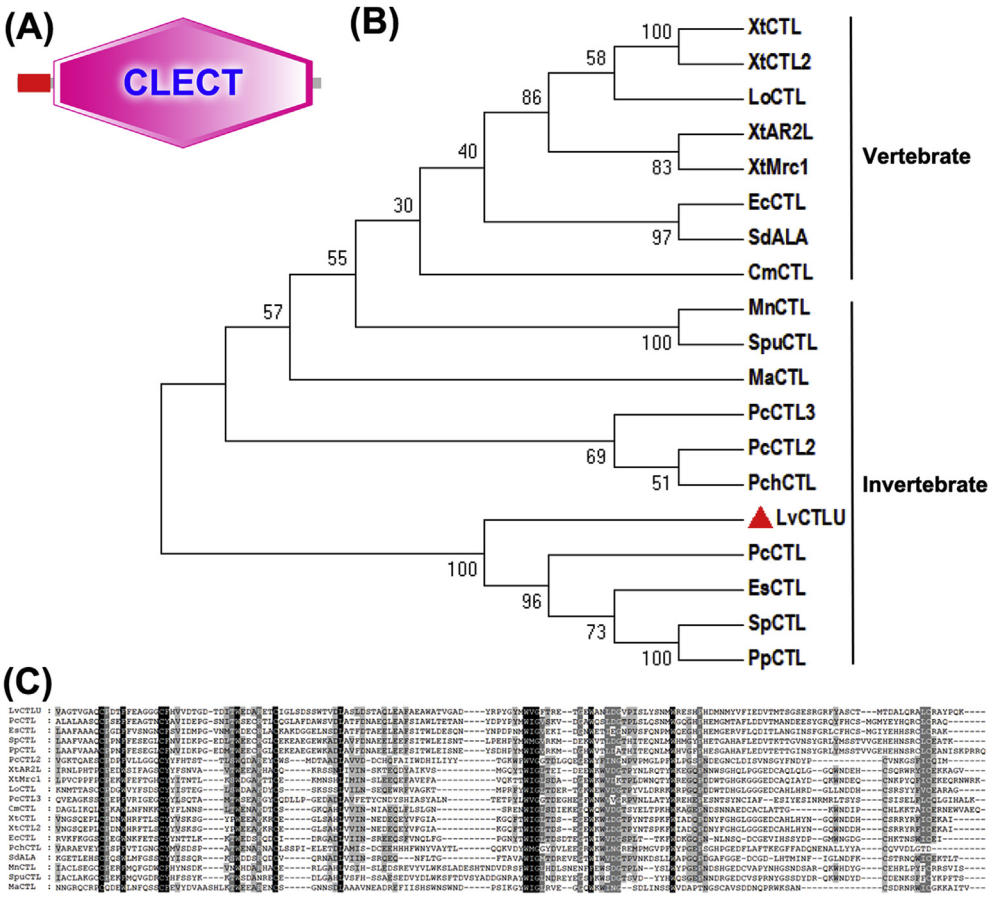

Fig. 2. Multiple sequence alignment of the CTL proteins CLETC domain, and phylogenetic analysis of the CTL proteins. (A) Schematic representation of the structural domain of *L. vannamei* LvCTLU protein. (B) Phylogenetic tree of CTLs: XtCTL, *Xenopus tropicalis* CTL (GenBank accession No. XP_012815689); XtCTL2, *Xenopus tropicalis* CTL2 (GenBank accession No. NP_001011225); LoCTL, *Lepisosteus oculatus* CTL (GenBank accession No. XP_006627571); XtAR2L, *Xenopus tropicalis* AR2L (GenBank accession No. XP_017945793); XtMrc1, *Xenopus tropicalis* Mrc1 (GenBank accession No. AAH77648); EcCTL, *Esox lucius* CTL (GenBank accession No. NP_001290572); SdALA, *Seriola dumerili* ALA (GenBank accession No. XP_022612965); CmCTL, *Callorhinchus milii* CTL (GenBank accession No. XP_007907578); MnCTL, *Mesocentrotus nudus* CTL (GenBank accession No. ACV41410); SpuCTL, *Strongylocentrotus purpuratus* CTL (GenBank accession No. XP_003725900); MaCTL, *Mastacembelus armatus* CTL (GenBank accession No. XP_026172418); PcCTL3, *Procambarus clarkii* CTL3 (GenBank accession No. ADK27312); PcCTL2, *Procambarus clarkii* CTL2 (GenBank accession No. AGL46986); LvCTLU, *L. vannamei* LvCTLU (GenBank accession No. MK952741); PchCTL, *Penaeus chinensis* CTL (GenBank accession No. ACJ06431); PcCTL, *Procambarus clarkii* CTL (GenBank accession No. AGI92548); EsCTL, *Eriocheir sinensis* CTL (GenBank accession No. ADH53777); SpCTL, *Scylla paramamosain* CTL (GenBank accession No. AHM25604); PpCTL, *Portunus pelagicus* CTL (GenBank accession No. ABM65757). (C) Multiple sequence alignment of the CLETC domain in CTL proteins. The result shows a high homology of amino acid sequences at this domain.

2.6. Analysis of phagocytosis using flow cytometry

Phagocytic activity was measured as previously described [23]. Briefly, shrimp were injected with dsLvCTLU or dseGFP. At 48 h post-injection, hemocytes were extracted from healthy shrimp and washed three times with 2 × Leibovitz's L-15 medium (Gibco, USA). Washed hemocytes were then incubated with FITC-labeled *V. parahaemolyticus* at a ratio of 1 hemocyte:100 bacterial cells. After incubation at 28 °C for 1 h, FITC signals and forward scatter (FSC) values in the hemocytes were measured using cytometry. The FSC threshold was determined by detecting free FITC-labeled *V. parahaemolyticus* in order to eliminate the influence of cell debris and bacteria, and the fluorescence boundary was set based on levels of self-fluorescence in untreated hemocytes. A total of 150,000 events were detected for each sample.

2.7. Cumulative mortality test LvCTLU-knockdown shrimp following WSSV or V. parahaemolyticus infection

The gene expression level of *LvCTLU* was reduced using RNA interference (RNAi) mediated by sequence-specific dsLvCTLU, and real-time RT-PCR was performed 72 h after dsRNA injection to measure RNAi efficiency in haemocytes of shrimp. *LvEF1a* was used as the internal control. To determine the cumulative mortality of *LvCTLU*-knockdown shrimp, healthy shrimp (n = 50 per group) were injected at the second abdominal segment with 6 μg of dsLvCTLU, dseGFP, or PBS. Approximately 48 hpi, shrimp were injected with 50 μL of WSSV inoculum or *V. parahaemolyticus*.

3. Results

3.1. LvCTLU cloning and sequence analysis

The full-length cDNA of *LvCTLU* was 1324 bp, including a 151 bp 5′-untranslated region (UTR) and a 663 bp 3′-UTR with a poly (A) tail (Fig. 1). The open reading frame (ORF) of *LvCTLU* was 510 bp, encoding a putative protein of 170 aa with a calculated molecular weight of 18.82 kDa (Fig. 1). Conserved domain analysis using SMART (http://smart.embl-heidelberg.de/) indicated that *LvCTLU* carried a putative signal peptide at the amino end. In addition, the CTL or carbohydrate-recognition (CLETC) domain was almost as long as the entire polypeptide (Fig. 2A).

3.2. Phylogenetic analysis

To investigate the relationships among LvCTLU and its homologs, a multiple sequence alignment was constructed (Fig. 2C); analysis showed that LvCTLU was highly similar to other CTLs in invertebrates and some lower vertebrates (Fig. 2B). A phylogenetic tree was generated using the neighbor-joining (NJ) method. In the resultant phylogeny, the CTLs and associated proteins fell into three classes (Fig. 3B): class 1 contained lower vertebrate and invertebrate CTLs (XtCTL, XtCTL2, LoCTL, XtAR2L, XtMrc1, EcCTL, SdALA, CmCTL, McCTL, SpuCTL, and MaCTL); class 2 contained the three shrimp CTLs (PcCTL2, PcCTL3, and PchCTL); and class 3 contained five crustacean CTLs (LvCTLU, EsCTL, SpCTL, and PpCTL). Although asialoglycoprotein receptor 2-like (XtAR2L), XtMrc1, and antigen-like protein A (SdALA) have not previously been specifically identified as CTLs, these proteins

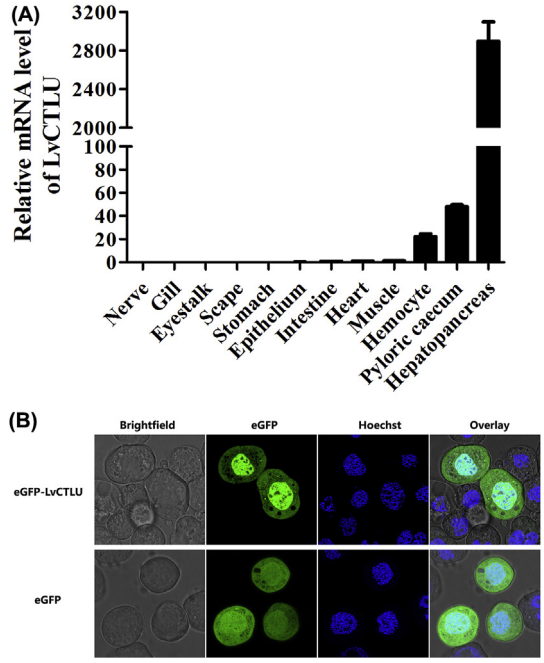

Fig. 3. Expression profile of *LvCTLU* in tissues and subcellular localization of LvCTLU. (A) Total RNA extracted from different tissues were reverse-transcribed to cDNAs to serve as templates. Relative expression levels were normalized to *LvEF1α*. The results are based on three independent experiments and expressed as mean values ± S.D. Statistical significance was determined by one-way ANOVA. Bars with different letters indicate statistical differences ($p < 0.05$). (B) S2 cells were transfected with pAC-eGFP-LvCTLU expression plasmids. At 48 h post-transfection, the cells were stained with Hoechst 33258 and visualized with confocal microscope.

contained the CLECT domain.

3.3. *LvCTLU was constitutively transcribed in various tissues and was localized in the cytoplasm*

Real-time RT-PCR analysis indicated that *LvCTLU* was expressed in all tissues examined herein. *LvCTLU* was extremely highly expressed in the shrimp hepatopancreas: ~2390-fold greater than the expression level in the nerve. *LvCTLU* was also highly expressed in pyloric caecum and hemocytes, 48- and 22-fold higher than the expression level in the nerve, respectively (Fig. 3A).

The subcellular locations of proteins may provide essential clues to their functions. To better understand the functions of LvCTLU, we determined the subcellular distribution of LvCTLU-eGFP in SF9 cells (Fig. 3B). We found that LvCTLU-eGFP was widely distributed in cytoplasm and was possibly somewhat aggregated in nucleus. In contrast, unfused eGFP was uniformly distributed (Fig. 3B).

3.4. *LvCTLU expression was induced by WSSV or V. parahemolyticus infection*

The expression levels of *LvCTLU* were measured using real-time RT-PCR assays. The gene expression levels of *LvCTLU* in the gill and hepatopancreas increased from 36 to 96 h post WSSV injection. In the intestine, *LvCTLU* expression began to increase from 6 h post WSSV infection, peaking at 36 hpi (at ~9.1-fold greater than the expression level of the control; Fig. 4A).

In the gill, *LvCTLU* expression increased from 24 h post *V. parahemolyticus* infection, peaking at 48 hpi (4.7-fold greater than the expression level of the control). In the intestine, *LvCTLU* was expressed from 12 hpi and peaked at 48 hpi (7.2-fold greater than the expression level of the control). In the hepatopancreas, *LvCTLU* was expressed from 24 hpi and peaked at 48 hpi (4.7-fold greater than the expression level of the control; Fig. 4B).

3.5. *Regulation of microbe agglutination and phagocytosis by LvCTLU*

The agglutinating activity of the recombinant LvCTLU protein was investigated using FITC-labeled microbes. The gram-negative microbe *V. parahaemolyticus* and the gram-positive bacteria *S. agalactiae* were agglutinated after incubation with 60 μg/mL LvCTLU in the presence of Ca^{2+}, but agglutination was not observed when Ca^{2+} was chelated with EDTA. This suggested that LvCTLU-mediated agglutination was Ca^{2+}-dependent (Fig. 5A). The influence of LvCTLU on hemocyte phagocytosis was investigated using flow cytometry. We observed less hemocyte-induced phagocytosis of *V. parahaemolyticus* in the LvCTLU-

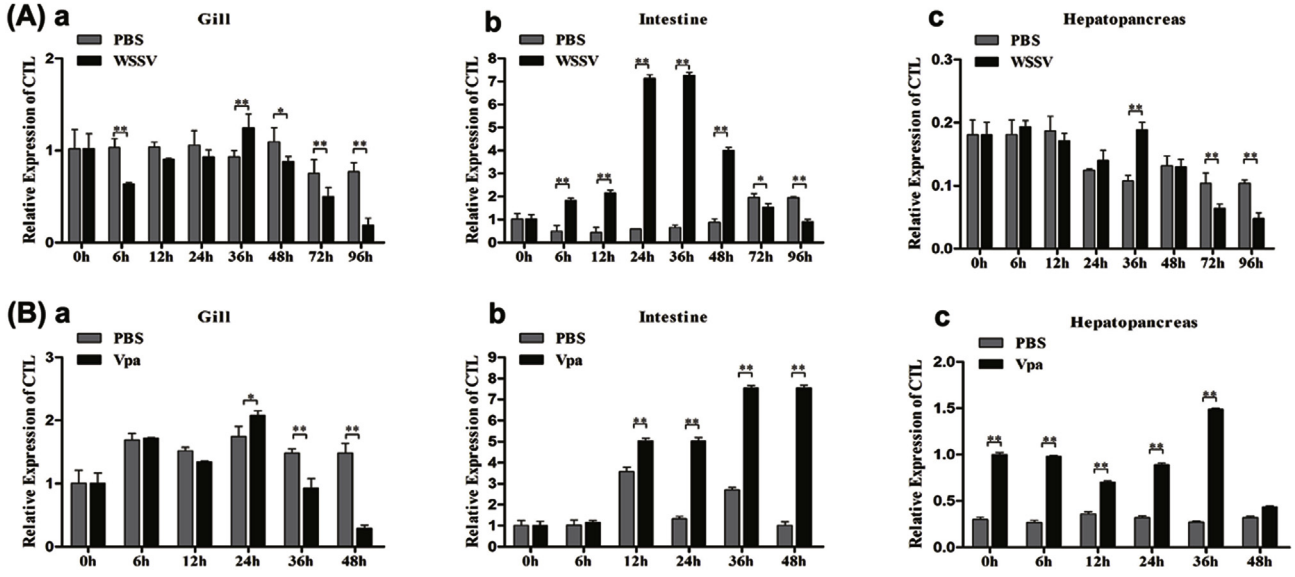

Fig. 4. Microbes aggregation and phagocytosis functions of LvCTLU. FITC-labeled *V. parahemolyticus* (1×10^6 CFU/mL) and *S. aureus* (1×10^6 CFU/mL) were treated with purified recombinant LvCTLU protein (2 μg) for 1 h in the presence of 10 mM $CaCl_2$ with or without EDTA at room temperature and examined under fluorescence microscopy. NC, Negative control (the control pET32a + expression protein). (B) Effects of LvCTLU on phagocytosis of hemocytes. The phagocytic activity of hemocytes from dsLvCTLU and dseGFP treated shrimp against FITC-labeled *V. parahaemolyticus* analyzed by flow cytometry.

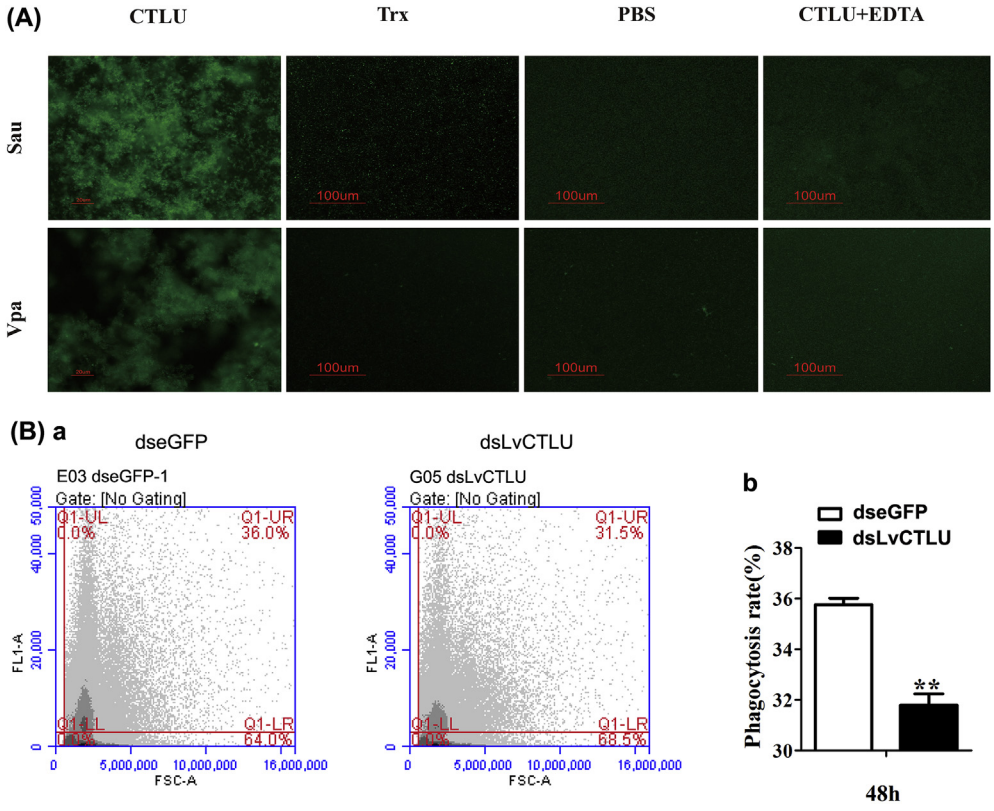

Fig. 5. Expression of *LvCTLU* in gills, intestine and hepatopancreas of immune challenged shrimps. (A) The mRNAs were collected at 0, 6, 12, 24, 36, 48, 72 and 96 h after WSSV infection; and (B) at 0, 6, 12, 24, 36 and 48 h after *V. parahemolyticus* infection. The relative expression of *LvCTLU* upon WSSV or *V. prahaemolyticus* infection were normalized with *LvEF1α* and compared against time zero. The bars represent the mean values ± S.D. of three replicates. The statistical significance was calculated using Student's *t*-test (*indicates $p < 0.05$, **indicates $p < 0.01$).

knockdown shrimp as compared to the control (Fig. 5B).

3.6. Knockdown of LvCTLU increased the cumulative mortality of V. parahemolyticus-infected, but not WSSV-infected, shrimp

As the results of real-time RT-PCR showed, dsLvCTLU but not dseGFP injection significantly reduced expression of *LvCTLU* in *L. vannamei* haemocytes at 72 h post dsRNA injection (Fig. 6A). To better understand the anti-pathogen properties of *LvCTLU*, we investigated the cumulative mortality of wild-type and *LvCTLU*-knockdown *L. vannamei* following *V. parahemolyticus* infection. In the infected shrimp injected with dsLvCTLU, cumulative mortality was 7%, 50%, and 97% at 8, 12, and 20 hpi, respectively (Fig. 6A). In the infected shrimp injected with dsLveGFP, cumulative mortality was 4%, 33%, and 50% at 8, 12, and 20 hpi, respectively (Fig. 6B).

In contrast, the knockdown of *LvCTLU* did not seem to significant impact the cumulative mortality of WSSV-infected shrimp. In the WSSV-infected shrimp injected with dsLvCTLU, cumulative mortality was 55%, 65%, and 80% at 36, 44, and 52 hpi, respectively (Fig. 6C). In the WSSV-infected shrimp injected with dsLveGFP, cumulative mortality was 30%, 40%, and 55% at 36, 44, and 52 hpi, respectively (Fig. 6C).

3.7. LvCTLU was induced by UPR

We constructed pGL4-LvCTLU and pGL4-LvCTLUmATF/CRE vectors, carrying the 669 bp promoter region of LvCTLU containing either the putative ATF/CRE binding motif (−575 to 567 bp; tcacgtca) or the mutant one [Fig. 7A (a)]. The dual-luciferase reporter assay indicated that the over-expression of LvXBP1s significantly increased pGL3-LvCTLU activity but had no significant impact on pGL4-LvCTLUmATF/CRE activity [Fig. 7A (b)]. In shrimp injected with dsLvBip, which activates shrimp UPR, *LvCTLU* was upregulated in the hemocytes from 24 hpi and continued to increase throughout the remainder of the experiment. At 96 h post dsLvBip injection, *LvCTLU* expression in the shrimp hemocytes was about 6.59-fold greater than that of the control. In contrast, *LvCTLU* expression levels remained relatively stable in shrimp injected with dseGFP (Fig. 7B).

4. Discussion

CTLs are known to recognise specific carbohydrate structures, act as pattern recognition receptors (PRRs), and regulate a diverse range of physiological functions, especially those associated with the immune response. Yet few studies have investigated the relationship between CTLs and the UPR. In this study, a novel CTL (LvCTLU) was cloned from *L. vannamei*. This CTL had Ca^{2+}-dependent bacterial agglutinating properties. Moreover, *LvCTLU* expression was regulated by LvXBP1s, which is the key transcription factor of the UPR, suggesting that *LvCTLU* is a downstream gene of the *L. vannamei* UPR.

Members of the CTL family possess at least one carbohydrate recognition domain (CRD), which mediates carbohydrate-binding activity and has two highly conserved disulfide bonds [24]. Our multiple sequence alignment suggested that LvCTLU could form two disulfide bonds as this protein carries four cysteinyl residues in its CRD. In addition, Predictprotein.com [25] analysis suggested that two disulfide bonds were likely to form within the LvCTLU CRD, with the first disulfide bond between C20 and C32, and the second between C52 and C163.

Although not all the CRD-containing proteins belong to the CTL family, CTL proteins are always Ca^{2+}-dependent because the specific amino acid residues that coordinate Ca^{2+} and bind to sugar hydroxyl groups are conserved [7]. This key functional aspect distinguishes CTLs from other types of lectins. Here, the microbe agglutinating activity of LvCTLU was Ca^{2+}-dependent, indicating that this protein falls into the CTL family.

CTL proteins are known to be associated with immune functions, particularly antibacterial activities. CTL antibacterial functions primarily have to do with binding the carbohydrates of the host or of the intruders [26]. Some CTLs act as signal transduction molecules,

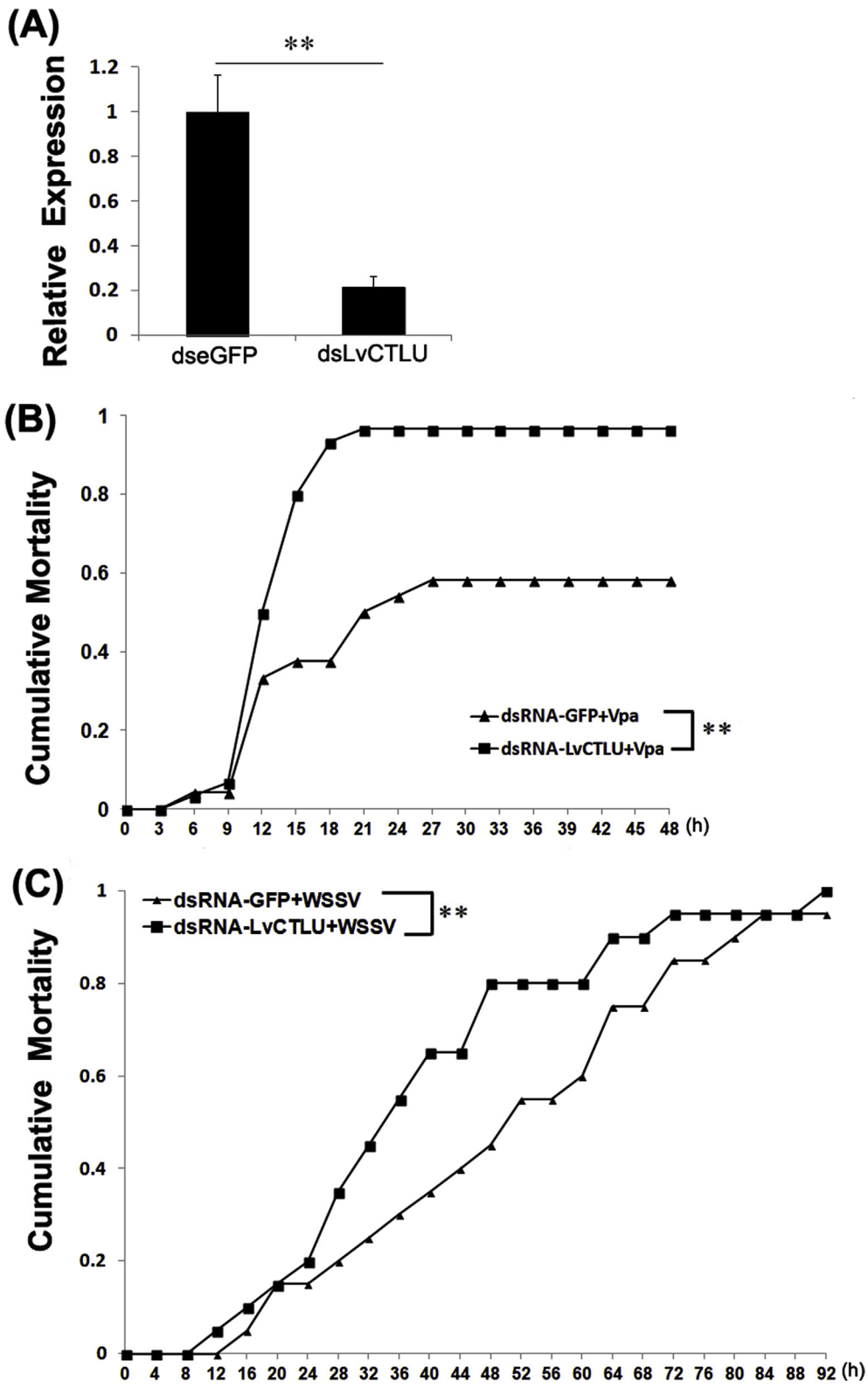

Fig. 6. Cumulative mortality following treatment with dsLvCTLU plus immune challenged. (A) Real-time RT-PCR analysis of gene expression of *LvCTLU,* the internal control was *LvEF1α*. Samples were taken 72 h after injection with indicated dsRNA; Shrimps ($n = 50$) were injected intramuscularly with dseGFP (control) or dsLvLvCTLU. At 48 h after the initial injection, shrimps were infected with *V. parahemolyticus* (B) or WSSV (C). Cumulative mortality was recorded every 3 or 4 h. Differences in mortality levels between treatments were analyzed by *Kaplane-Meier* plot (log-rank X^2 test). Significant differences in *L. vannamei* mortality were marked with asterisks (**indicates $p < 0.01$).

mediating immune signal by interacting with the glycosyl groups of glycoproteins. For example, CTL interacts with the transmembrane glycoprotein receptor *β*-integrin to enhance hemocytic encapsulation in the cotton bollworm, *Helicoverpa armigera* [27]. In addition, macrophage inducible CTL (Mincle) recognizes the glycosylated surface (S)-layer of *Tannerella forsythia* and may play a critical role in regulating the host immune response to this bacterium [28]. Here, LvCTLU regulated the microbe agglutination activity of shrimp hemocytes, suggesting that LvCTLU might bind to the carbohydrates on the surfaces of the invading bacteria. Furthermore, LvCTLU also participated in the regulation of phagocytic activity. As report, CTLs could be involved in phagocytic in several ways. CTLs, such as Dectin-1 can directly recognise pathogen associated molecular patterns (PAMPs) on the surface of microbes and mediate phagocytosis [29]. Alternatively, soluble CTLs,

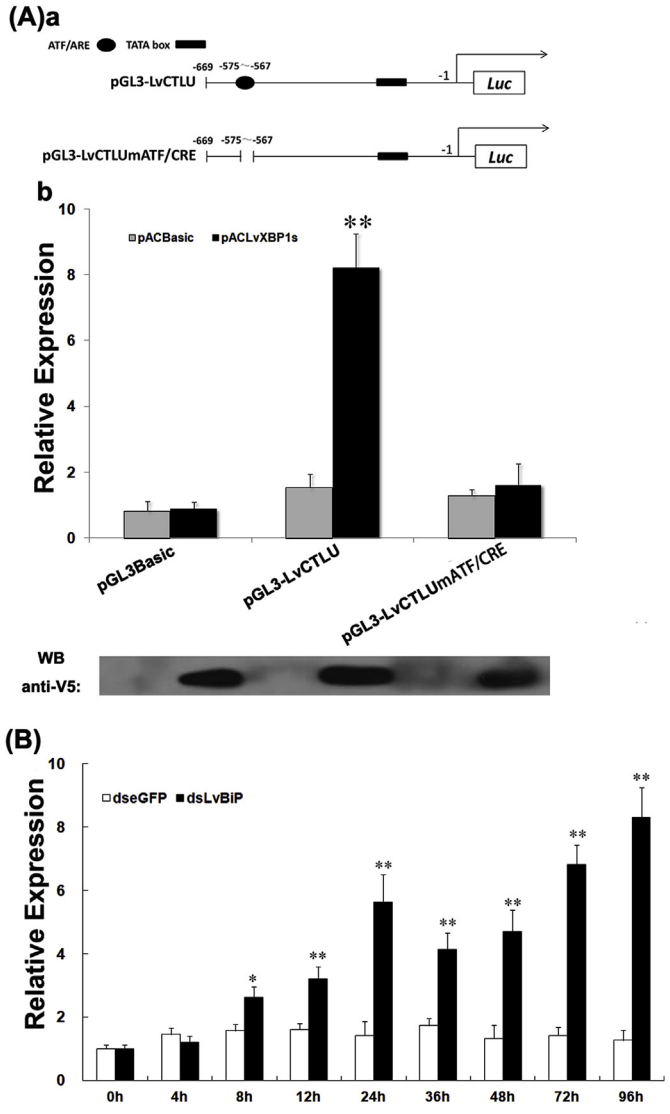

Fig. 7. *LvCTLU* is regulated by UPR. [A (a)] Schematic diagram of *LvCTLU* promoter regions in the luciferase reporter gene constructs. The mutant promoters of *LvCTLU* with the ATF/CRE site was indicated. −1 indicates 1 bp before the translation initiation site. Luc denotes the firefly luciferase reporter gene. The putative ATF/CRE site is indicated by elliptical boxes, and the mutanted site is indicated by open boxes. [A (b)] The relative luciferase activity of pGL3B-LvCTLU and pGL3B-LvCTLUmATF/CRE, which that ATF/CRE in promoter of *LvCTLU* is mutanted. The bars indicate mean values ± S.D. of the luciferase activity ($n = 3$). (B) Activation of the *LvCTLU* promoter by LvXBP1s. The mRNAs were collected at v0, 4, 8, 12, 24, 36, 48, 72 and 96 h after dsLvBip or dseGFP injection. Then expression levels of *LvCTLU* at various timeswere measured using real-time RT-PCR. The statistical significance was calculated using Student's *t*-test (** indicates $p < 0.01$).

such as mannose-binding lectin (MBL) can interact directly with pathogens to promote opsonisation of the microbe, which can subsequently be phagocytosed via specific receptors [30]. Furthermore, some CTLs can activate complement leading to its deposition on the microbial surface and phagocytosis mediated by complement receptors [31]. In addition, CTLs can cause upregulation of other phagocytic receptors, independently of their binding to the microbe. For example, MBL upregulation of scavenger receptor A (SR-A) [31]. Yet how LvCTLU is engaged in phagocytosis still unclear. These results indicated that LvCTLU might be a pattern recognition receptor, recognizing microorganisms and mediating the immune response in *L. vannamei*.

Similarly, CTLs also elicit and shape the adaptive immune response to viral invasion to inhibit viral spread; some viruses exploit CTLs in order to enter host immune cells and avoid immune recognition. For example, chicken lung lectin is a functional CTL that inhibits the haemagglutination of the influenza A virus [32]. In contrast, the human immunodeficiency virus-1 envelope triggers polyclonal Ig class switch recombination via a CD40-independent mechanism that involves B cell-activating factors and CTL receptors [33]. Here, we showed that LvCTLU was involved not only in the antibacterial response but also in the anti-viral (WSSV) response. This was consistent with several previous studies demonstrating that crustacean CTLs act as both antivirals and antibacterials, such as a CTL harboring an additional low-density lipoprotein receptor (LDLR) class A domain (LdlrCTL) in *L. vannamei*, as well as PcLEC6 and PcLT in *Procambarus clarkii* [14,34,35].

In addition to pathogens, shrimp are also subject to various environmental stressors. The UPR, which is initiated in the ER, is a mechanism used by eukaryotic cells to resist stresses [36]. The UPR is a cascade of responses that prevent the accumulation of unfolded or misfolded proteins in the ER lumen. This mechanism is highly conserved from human to yeast [37,38]. The UPR contributes to cell survival during ER-stress by enhancing the protein folding capacity of the ER [39]. Previously, we showed that the UPR is important for environmental stress resistance in shrimp [18–20]. Shrimp CTLs may also be involved in resistance to environmental stress. For example, CTLs were expressed in response to bacterial infection and ammonia nitrogen stress in tiger shrimp [40]. In addition, several transcriptional and histological analyses have indicated that CTLs may be involved in shrimp environmental stress responses [16,41,42]. Here, we demonstrated that *LvCTLU* was a downstream gene of the UPR and was regulated by LvXBP1s. These results indicated that *LvCTLU* might also play a vital role in the environmental stress response. However, the specific functions of *LvCTLU* during the stress response require further study.

In summary, we cloned a *CTL* gene from *L. vannamei* (*LvCTLU*) with both antibacterial and antiviral properties. Moreover, the expression of this gene was induced by the UPR and regulated by LvXBP1.

Acknowledgements

This research was supported by National Natural Science Foundation of China (31472301); Guangdong Natural Science Funds for Distinguished Young Scholar (2015A030306030); Special Support Program of Science and Technology Innovation of Young Talents (2015TQ01N220); Open Project Fund of Guangdong Provincial Key Laboratory for Healthy and Safe Aquaculture(GDKLHSA0802). The nucleotide sequences of *LvCTLU* had been submitted to NCBI database and with GenBank accession No. MK952741.

References

[1] W.J. Peumans, E.J. Van Damme, Lectins as plant defense proteins, Plant Physiol. 109 (1995) 347–352.
[2] D.B. AbuSamra, P. Argüeso, Lectin-glycan interactions in corneal infection and inflammation, Front. Immunol. 9 (2018) 2338.
[3] H. Ghazarian, B. Idoni, S.B. Oppenheimer, A glycobiology review: carbohydrates, lectins and implications in cancer therapeutics, Acta Histochem. 113 (2011) 236–247.
[4] T. Fujita, Evolution of the lectin-complement pathway and its role in innate immunity, Nat. Rev. Immunol. 2 (2002) 346–353.
[5] C.P. Mason, A.W. Tarr, Human lectins and their roles in viral infections, Molecules 20 (2015) 2229–2271.
[6] S. Yamasaki, M. Matsumoto, O. Takeuchi, T. Matsuzawa, E. Ishikawa, M. Sakuma, et al., C-type lectin Mincle is an activating receptor for pathogenic fungus, *Malassezia*, Proc. Natl. Acad. Sci. U.S.A. 106 (2009) 1897–1902.
[7] A.N. Zelensky, J.E. Gready, The C-type lectin-like domain superfamily, FEBS J. 272 (2005) 6179–6217.
[8] Ac Mistry, S. Honda, S. Hirose, Structure, properties and enhanced expression of galactose-binding C-type lectins in mucous cells of gills from freshwater Japanese eels (Anguilla japonica), Biochem. J. 360 (2001) 107–115.
[9] M.E. Taylor, K. Drickamer, Structure-Function Analysis of C-type Animal Lectins. Methods in Enzymology, Academic Press, 2003, pp. 3–16.
[10] C.D. Collard, A. Väkevä, M.A. Morrissey, A. Agah, S.A. Rollins, W.R. Reenstra, et al.,

Complement activation after oxidative stress: role of the lectin complement pathway, Am. J. Clin. Pathol. 156 (2000) 1549–1556.
[11] N. Moniaux, M. Darnaud, K. Garbin, A. Dos Santos, C. Guettier, D. Samuel, et al., The Reg3α (HIP/PAP) lectin suppresses extracellular oxidative stress in a murine model of acute liver failure, PLoS One 10 (2015) e0125584.
[12] T. Tatsuta, M. Hosono, Y. Miura, S. Sugawara, Y. Kariya, S. Hakomori, et al., Involvement of ER stress in apoptosis induced by sialic acid-binding lectin (lectzyme) from bullfrog eggs, Int. J. Oncol. 43 (2013) 1799–1808.
[13] X. Zhao, H. Yu, L. Kong, Q. Li, Transcriptomic responses to salinity stress in the pacific oyster *Crassostrea gigas*, PLoS One 7 (2012) e46244.
[14] X.W. Zhang, X. Man, X. Huang, Y. Wang, Q.S. Song, K.M. Hui, et al., Identification of a C-type lectin possessing both antibacterial and antiviral activities from red swamp crayfish, Fish Shellfish Immunol. 77 (2018) 22–30.
[15] W. Senghoi, P. Runsaeng, P. Utarabhand, FmLC5, a putative galactose-binding C-type lectin with two QPD motifs from the hemocytes of *Fenneropenaeus merguiensis* participates in shrimp immune defense, J. Invertebr. Pathol. 150 (2017) 136–144.
[16] H. Guo, J.A. Xian, A.L. Wang, Analysis of digital gene expression profiling in hemocytes of white shrimp *Litopenaeus vannamei* under nitrite stress, Fish Shellfish Immunol. 56 (2016) 1–11.
[17] X. Lu, S. Luan, P. Dai, X. Meng, B. Cao, K. Luo, et al., iTRAQ-based comparative proteome analysis for molecular mechanism of defense against acute ammonia toxicity in Pacific White shrimp *Litopenaeus vannamei*, Fish Shellfish Immunol. 74 (2018) 52–61.
[18] Y.H. Chen, L. Zhao, L.R. Pang, X.Y. Li, S.P. Weng, J.G. He, Identification and characterization of Inositol-requiring enzyme-1 and X-box binding protein 1, two proteins involved in the unfolded protein response of *Litopenaeus vannamei*, Dev. Comp. Immunol. 38 (2012) 66–77.
[19] K. Yuan, F.H. Yuan, H.H. He, H.T. Bi, S.P. Weng, J.G. He, et al., Heat shock 70 kDa protein cognate 5 involved in WSSV toleration of *Litopenaeus vannamei*, Dev. Comp. Immunol. 72 (2017) 9–20.
[20] X.Y. Li, L.R. Pang, Y.G. Chen, S.P. Weng, H.T. Yue, Z.Z. Zhang, et al., Activating transcription factor 4 and X box binding protein 1 of *Litopenaeus vannamei* transcriptional regulated white spot syndrome virus genes *Wsv023* and *Wsv083*, PLoS One 8 (2013) e62603.
[21] Y.H. Chen, X.T. Jia, L. Zhao, C.Z. Li, S. Zhang, Y.G. Chen, et al., Identification and functional characterization of Dicer2 and five single VWC domain proteins of *Litopenaeus vannamei*, Dev. Comp. Immunol. 35 (2011) 661–671.
[22] Y.H. Chen, F.H. Yuan, H.T. Bi, Z.Z. Zhang, H.T. Yue, K. Yuan, et al., Transcriptome analysis of the unfolded protein response in hemocytes of *Litopenaeus vannamei*, Fish Shellfish Immunol. 54 (2016) 153–163.
[23] S.W. Niu, L.W. Yang, H.L. Zuo, J.F. Zheng, S.P. Weng, J.G. He, et al., A chitinase from pacific white shrimp *Litopenaeus vannamei* involved in immune regulation, Dev. Comp. Immunol. 85 (2018) 161–169.
[24] A.J. Day, The C-type carbohydrate recognition domain (CRD) superfamily, Biochem. Soc. Trans. 22 (1994) 83–88.
[25] B. Rost, G. Yachdav, J. Liu, The PredictProtein server, Nucleic Acids Res. 32 (2004) W321–W326.
[26] A. Cambi, M. Koopman, C.G. Figdor, How C-type lectins detect pathogens, Cell Microbiol. 7 (2005) 481–488.
[27] P. Wang, X.R. Zhuo, L. Tang, X.S. Liu, Y.F. Wang, G.X. Wang, et al., C-type lectin interacting with β-integrin enhances hemocytic encapsulation in the cotton bollworm, *Helicoverpa armigera*, Insect Biochem. Mol. Biol. 86 (2017) 29–40.
[28] S. Chinthamani, R.P. Settem, K. Honma, J.G. Kay, A. Sharma, Macrophage inducible C-type lectin (Mincle) recognizes glycosylated surface (S)-layer of the periodontal pathogen Tannerella forsythia, PLoS One 12 (2017) e0173394.
[29] B.N. Gantner, R.M. Simmons, D.M. Underhill, Dectin-1 mediates macrophage recognition of Candida albicans yeast but not filaments, EMBO J. 24 (2005) 1277–1286.
[30] N. Brouwer, K.M. Dolman, M. van Houdt, M. Sta, D. Roos, T.W. Kuijpers, Mannose-binding lectin (MBL) facilitates opsonophagocytosis of yeasts but not of bacteria despite MBL binding, J. Immunol. 180 (2008) 4124–4132.
[31] A.M. Kerrigan, G.D. Brown, C-type lectins and phagocytosis, Immunobiology 214 (2009) 562–575.
[32] A. Hogenkamp, N. Isohadouten, S.S.N. Reemers, R.A. Romijn, W. Hemrika, M.R. White, et al., Chicken lung lectin is a functional C-type lectin and inhibits haemagglutination by influenza A virus, Vet. Microbiol. 130 (2008) 37–46.
[33] B. He, X. Qiao, P.J. Klasse, A. Chiu, A. Chadburn, D.M. Knowles, et al., HIV-1 envelope triggers polyclonal Ig class switch recombination through a CD40-independent mechanism involving BAFF and C-type lectin receptors, J. Immunol. 176 (2006) 3931–3941.
[34] Z.W. Liang, L.W. Yang, J.F. Zheng, H.L. Zuo, S.P. Weng, J.G. He, et al., A low-density lipoprotein receptor (LDLR) class A domain-containing C-type lectin from *Litopenaeus vannamei* plays opposite roles in antibacterial and antiviral responses, Dev. Comp. Immunol. 92 (2019) 29–34.
[35] D.D. Chen, X.L. Meng, J.P. Xu, J.Y. Yu, M.X. Meng, J. Wang, PcLT, a novel C-type lectin from *Procambarus clarkii*, is involved in the innate defense against Vibrio alginolyticus and WSSV, Dev. Comp. Immunol. 39 (2013) 255–264.
[36] M. Schroder, R.J. Kaufman, ER stress and the unfolded protein response, Mutat. Res. 569 (2005) 29–63.
[37] X. Shen, R.E. Ellis, K. Lee, C.Y. Liu, K. Yang, A. Solomon, et al., Complementary signaling pathways regulate the unfolded protein response and are required for *C. elegans* development, Cell 107 (2001) 893–903.
[38] M. Dragosits, J. Stadlmann, A. Graf, B. Gasser, M. Maurer, M. Sauer, et al., The response to unfolded protein is involved in osmotolerance of *Pichia pastoris*, BMC Genomics 11 (2010) 207.
[39] S.J. Marciniak, D. Ron, Endoplasmic reticulum stress signaling in disease, Physiol. Rev. 86 (2006) 1133–1149.
[40] Y.K. Qin, S.G. Jiang, J.H. Huang, F.L. Zhou, Q.B. Yang, S. Jiang, et al., C-type lectin response to bacterial infection and ammonia nitrogen stress in tiger shrimp (*Penaeus monodon*), Fish Shellfish Immunol. 90 (2019) 188–198.
[41] W.H. Gao, B.P. Tan, K.S. Mai, S.Y. Chi, H.Y. Liu, X.H. Dong, et al., Profiling of differentially expressed genes in hepatopancreas of white shrimp (*Litopenaeus vannamei*) exposed to long-term low salinity stress, Aquaculture 364–365 (2012) 186–191.
[42] H. Guo, C.X. Ye, A.L. Wang, J.A. Xian, S.A. Liao, Y.T. Miao, et al., Trascriptome analysis of the Pacific white shrimp *Litopenaeus vannamei* exposed to nitrite by RNA-seq, Fish Shellfish Immunol. 35 (2013) 2008–2016.